Journal of Applied Electrochemistry **30**: 35–41, 2000.

Impedance spectroscopy study of electrochromism in sputtered iridium oxide films

Th. PAUPORTÉ* and R. DURAND
Laboratoire d'Électrochimie et de Physico-chimie des Matériaux et des Interfaces, UMR CNRS-INPG 5631, ENSEEG, 1130 Rue de la Piscine, Domaine Universitaire, BP75, 38402 Saint Martin d'Hères, Cedex, France
*(*author for correspondence at Laboratoire d'Électrochimie et Chimie analytique, ENSCP, UMR 7575, 11 Rue P. et M. Curie, 75231 Paris Cedex 5, France; e-mail: pauporte@ext.jussieu.fr)*

Received 15 February 1999; accepted in revised form 20 May 1999

Key words: electrochromism, impedance spectroscopy, iridium oxide, proton insertion, sputtered film

Abstract

The a.c. impedance response of sputtered iridium oxide films (SIROFs) was studied at room temperature in 1 M H_2SO_4 between 1 mHz and 50 mHz. The spectra were recorded as a function of applied potential in the range of electrochromic properties from 0.0 to 1.0 V vs SCE and before and after an electrochemical treatment consisting of alternatively colouring and bleaching the electrode. The spectra were analysed with help of an equivalent circuit. Between 0.4 and 1.0 V, the spectra can be interpreted as due to electrochemical proton insertion in a single phased compound. From the data, hydrogen chemical diffusion coefficients with values ranging from 2×10^{-8} to $1.1 \times 10^{-7}\,cm^2\,s^{-1}$ are found. It is shown that this parameter increases fourfold after the cycling treatment and significantly decreases with the amount of inserted hydrogen. Below 0.4 V spectrum changes are observed over the intermediate frequency range studied, indicating some changes of the interfacial reactivity which remain to be clarified.

1. Introduction

Iridium oxide is an electrochromic compound with a transition from transparent to grey–black colour occurring with oxidation [1–20]. The main advantages of this system are a short response time, a good stability in various media and an operating potential range (between 0 and 1 V vs SCE) over which aqueous medium is stable. The three main routes for preparing electrochromic iridium oxide are (i) anodic films obtained by cycling iridium metal electrodes between appropriate potential boundaries [1–9], (ii) films directly prepared by reactive r.f. sputtering in an oxygen atmosphere [10–18] and (iii) electrodeposition [19, 20]. It is now accepted that the mechanism leading to the colour change in acidic media is a double charge injection: during oxidation ions are ejected from the film into the solution and electrons from the film into the conducting electrode substrate [12]. In acidic media some investigations by Gottesfeld and McIntyre favoured a proton mechanism [1, 2]. They were supported later by some analytical studies by XPS [5], RBS and nuclear reaction ion beam microanalysis technique [6] and by the study of the density change of the electrolyte near the interface by a probe beam deflection technique [8, 17]. The reaction generally admitted is

$$IrO_2 + yH^+ + ye^- \Leftrightarrow IrO_{2-y}(OH)_y \quad (1)$$

with y the insertion number of hydrogen. The reaction leads to a change in the oxidation state of iridium as shown by XPS [5] and recent XAS experiments [9, 18].

The structure of iridium oxide depends on the preparation method. Anodic iridium oxide films (AIROF) have been shown to be highly porous and hydrated [21], with a low density of $2\,g\,cm^{-3}$ compared to that of massive IrO_2 ($11.6\,g\,cm^{-3}$). The density of as deposited sputtered films (SIROF) is close to $10\,g\,cm^{-3}$. It significantly decreases down to $7.8\,g\,cm^{-3}$ after a few successive colour-bleach cycles (CB treatment) [12, 14]. This has been attributed to the expansion that accompanies the hydration of the film. The fast response of as-deposited SIROFs is generally attributed to its amorphous structure [15, 16]. Moreover, using an electrochromic seven segment digit display, Hackwood et al. [12] have shown that the CB treatment mentioned above gives rise to a decrease in the time response of SIROFs by one order of magnitude.

Only AIROFs have been investigated by impedance. Glarum and Marshall [4] have used an equivalent circuit including a capacitance in parallel with an element due to the electrical response of the porous film. They presented a model in which the mobile species was reduced lattice sites with a diffusion coefficient controlled by the hydrogen ion exchange current within the pores. Aurian-Blajeni et al. [7] have used a more classical equivalent circuit for modelling the experimen-

tal spectra including a double layer capacitance, a charge transfer resistance and a Warburg element (constant phase angle element (CPE) with α close to 0.5). The variations of the Warburg coefficients with potential were interpreted assuming that the rate limiting step is the electronic transfer in the poorly-conducting reduced film and hydrogen diffusion in the conducting oxidized state.

No impedance data are available in the literature on films deposited by sputtering, actually the simplest and most usual method for obtaining electrochromic iridium oxide films. In the present work the a.c. response in the potential range of electrochromism has been studied in acidic medium as a function of potential and before and after some tens of CB treatment of the film. The spectra have been simulated in terms of an equivalent circuit. The variations in the extracted double-layer capacitance, kinetic and transport parameters with potential and history are discussed. The results show a behaviour different from that reported with AIROFs, which is likely related to fundamental differences in film morphology and structure.

2. Experimental details

The electrodes were iridium oxide films, 59 nm in thickness, deposited by reactive r.f. sputtering in a O_2 plasma onto glass panes coated with a 300 nm thick electronically conducting film of fluorine doped SnO_2. The electrical contact on the coating layer was taken with a platinum clip. The electrodes were 1.1 cm wide with surface areas in contact with the solution ranging from 0.25 to 0.35 cm^2. Before each experiment, the electrode was rinsed successively with acetone, ethanol and high purity milliQ water. The solution was 1 M H_2SO_4, prepared from concentrated suprapur H_2SO_4 (Merck) and milliQ water. The reference electrode was a saturated calomel electrode (SCE) separated from the main cell compartment by a Luggin capillary. The counter electrode was a plate of titanium of large area (6 cm^2) covered with a layer of iridium oxide obtained by thermal decomposition of H_2IrCl_6 [22].

Cyclic voltammograms were recorded with an EG&G 273A potentiostat controlled with the commercial M270 software. The impedance measurements were performed with a 1287 electrochemical interface and a 1255 Solartron frequency response analyser controlled with the commercial Scribner Associates 'Z plot' software. The spectra were recorded between 1 MHz and 0.05 Hz, seven or fourteen points per decade were taken and the a.c. amplitude was 7 mV. They were fitted with the nonlinear least square fitting program 'Z view' and each point was weighted by its magnitude.

The results were obtained from the following experiment: a first spectrum was recorded at 0.64 V vs SCE, the rest potential of the as-deposited electrode after immersion in solution. Spectra were then recorded successively at 0.4, 1.0, 0.8 and 0.64 V after applying the potential a few minutes to allow equilibration. The electrode was subsequently cycled 30 times. The cycling treatment consisted in alternatively colouring and bleaching the film by applying 1 V and 0 V vs SCE respectively, for 1 s. According to Hackwoods et al. [12] after this treatment, the film reaches a steady state thickness. A set of impedance spectra was recorded afterwards at different potentials ranging between 0 and 1 V after equilibrium. The reproducibility of the results presented here has been checked with several electrodes.

3. Results and discussion

Figure 1 shows a typical cyclic voltammogram of SIROF between −0.2 and 1 V vs SCE (second cycle). The general shape is in agreement with that reported in the literature [11] and betrays a capacitive behaviour with a proportionality of the current to the scan rate (not shown).

3.1. *Impedance equivalent circuit*

Between 0.4 and 1 V vs SCE, either before or after the CB treatment, the general shapes of the impedance spectra were very similar. Figures 2(a) and (b) and 3(a) and (b) show typical impedance plot in the Bode and Nyquist representations, respectively. In the Figures the series resistance has been subtracted. The equivalent circuit used for experimental spectral analysis is presented in Figure 4. The curves simulated with the parameter values extracted from the fitting of the experimental spectra with the equivalent circuit of Figure 4 are reported in solid line in Figures 2 and 3. The series inductance is classically attributed to the connection wires between the electrochemical interface and the cell. A poor fit was achieved using a double layer capacitance in parallel with the faradaic impedance and a CPE varying with frequency like $Z_{CPE} = 1/T(j\omega)^{\alpha}$ has been used. As reported later, α was close to 0.75. R_{ct} is the charge transfer resistance. In the low frequency

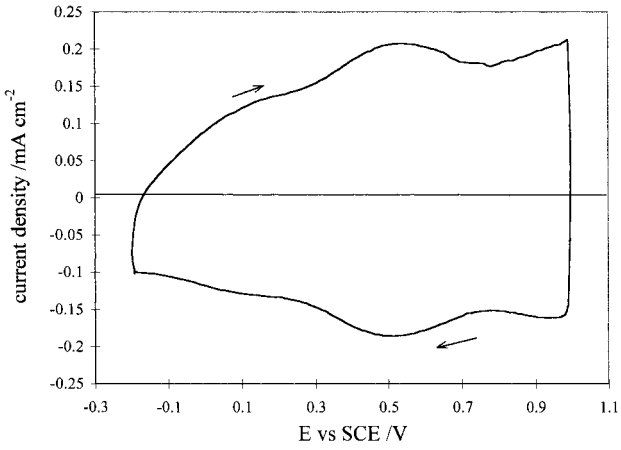

Fig. 1. Typical cyclic voltammogram of SIROF in 1 M H_2SO_4 measured at a rate of 10 mV s^{-1}.

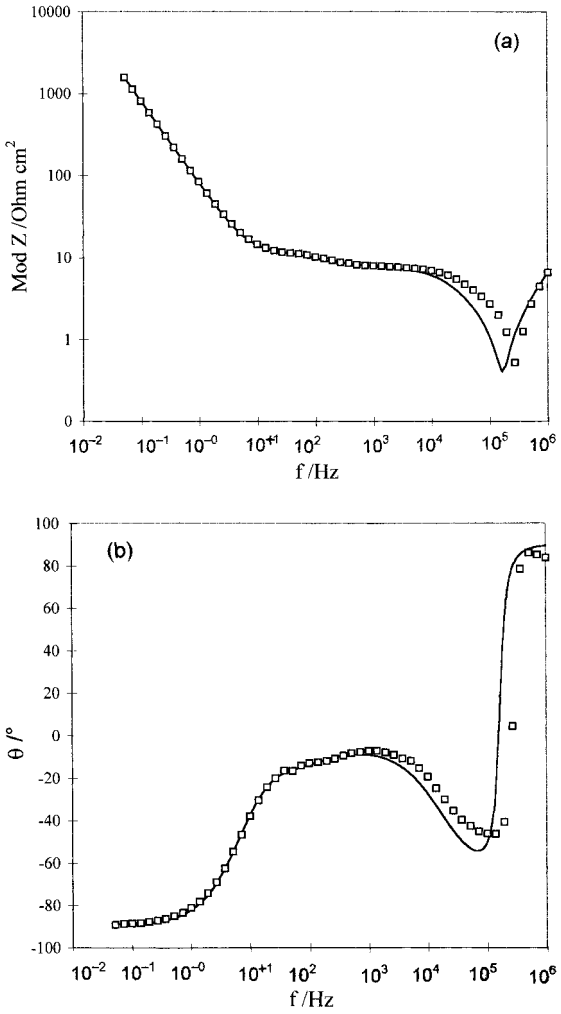

Fig. 2. Bode plots of a typical EIS spectrum recorded at 0.8 V after the CB treatment. R_s has been subtracted. Key: (□) experimental points (——) simulated curve after fitting with the equivalent circuit of Figure 4. (a) Z modulus against frequency; (b) theta phase against frequency.

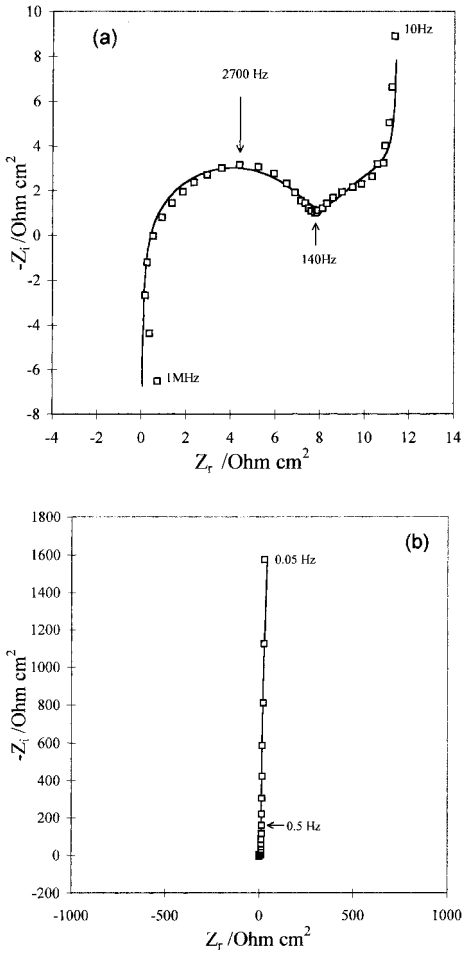

Fig. 3. Same data as in Figure 2 represented in a Nyquist plot. (a) High frequency range; (b) low frequency range.

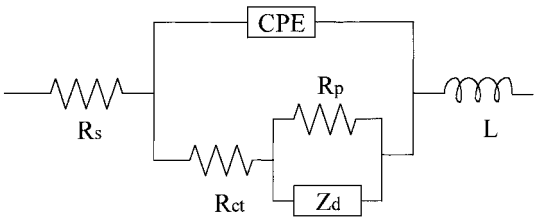

Fig. 4. Equivalent circuit used for fitting the experimental points.

range the spectra could be fitted with an element varying like $A\coth(j\omega u)^{1/2}/(j\omega u)^{1/2}$ and noted Z_d in the equivalent circuit. In the low frequency range, the plot did not give rise to a strictly vertical line and the fit was improved by adding a resistance, noted R_p, in parallel with this element. Experimental R_p values ranged between 3 and 6 kΩ cm^2.

The spectra are largely different from those reported with AIROF and cannot be explained by using the theoretical models developed for porous electrode [23]. Moreover, we have observed by scanning electron microscopy that the SIROF surface was very smooth both before and after a CB treatment with no feature above 0.03 μm. Sputtering likely gives an initial dense and amorphous layer. During cycling, water is introduced in the film and gives rise to an amorphous gel-like layer. In the following classical impedance models developed for smooth electrodes have been used for interpreting the results.

Z_d is most likely due to the restricted chemical diffusion of hydrogen in the film [24]. At high frequencies ($\omega > (4\tilde{D}_{H^+}/\ell^2)$), Z_d varies like a Warburg impedance, $W(j\omega)^{-1/2}$, with W the Warburg coefficient.

Another limiting case occurs at very low frequencies ($\omega < (\tilde{D}_{H^+}/4\ell^2)$):

$$Z_d = R_{in} + \frac{1}{j\omega C_{in}} \tag{2}$$

with

$$\frac{1}{C_{in}} = \frac{v_{IrO_2}\left(-\dfrac{dE}{dy}\right)}{FS\ell} \tag{3}$$

and

$$R_{in} = \frac{\ell v_{IrO_2}}{3FS\tilde{D}_H}\left(-\frac{dE}{dy}\right) \quad (4)$$

v_{IrO_2} is the molar volume of IrO_2. Between -0.2 and 1.1 V vs SCE, the lowest frequency data could be fitted with an equivalent circuit including $R_p \parallel C_{in}$ in series with a pure resistance. From the pseudocapacitance C_{in} and Equation 3, dE/dy can be calculated. In the following the ratio v_{IrO_2}/ℓ is supposed constant and equal to $3.8 \times 10^6\,cm^2\,mol^{-1}$ (with a molar mass of $224\,g\,mol^{-1}$ and a density of $10\,g\,cm^{-3}$).

As shown in Figure 2(a) and (b) the fitting curves achieved from the equivalent circuit of Figure 4 and presented with a solid line were more accurate at the lowest frequencies than at the highest. The parameter determined with the worse accuracy was T (with some $\pm 10\%$ error). With the other parameters, the accuracy was much better (some percent of relative error at maximum). Generally, impedance measurements are difficult to perform at high frequencies, mainly because the reference electrode and the Luggin capillary induce some parasitic signals.

Figure 5 shows that the spectra are rather different at potentials lower than 0.4 V: either before or after the CB treatment, the linear part over the intermediate frequency range of the study shows slopes smaller than 1. The corresponding impedance element varies approximately like $B(j\omega)^{-1/4}$. Moreover, at lower frequencies the spectra show an extended intermediate region before the onset of the pseudo-capacitance.

3.2. *Influence of potential and history on impedance parameters*

The charge transfer resistance, R_{ct}, was practically independent of potential and history with values of $0.9 \pm 0.2\,\Omega\,cm^2$. A small increase was claimed by Aurian-Blajeni et al. [7] with AIROF. The redox kinetics on these films is virtually independent of the applied potential. T higher than classical values reported for the double layer capacitance of smooth metal electrodes were found with a decrease of the parameter from 1.6×10^{-4} to $6.2 \times 10^{-5}\,S\,s^{\alpha}\,cm^{-2}$ between 0 and 1 V. On the other hand, their order of magnitude is not that expected for a very rough (porous) surface, in agreement with an earlier discussion. As already mentioned the uncertainty on T values was rather high. Nevertheless, a significant decrease in T with the CB treatment from 1.5×10^{-4} to 9×10^{-5} was observed, not attributable to a change of surface area (R_{ct} is constant with history). This may be due to some interfacial modification by the adsorption of some species. The α parameter was equal to 0.75 ± 0.05 with no significant change with potential and history.

The Nyquist plots clearly show, in accordance with the observations by cyclic voltammetry, that SIROFs have a capacitive behaviour at low frequencies. From Relation 3, C_{in} depends on dE/dy whose value is a function of the insertion isotherm.

$-dE/dy$ values are displayed in Figure 6 against potential and history. A slight decrease in the parameter is observed with cycling. The striking feature of the curve is a significant increase at the lowest potentials studied. By integration, we have built the iridium valency versus E curve extracted from impedance data (Figure 7). XAS experiments have shown that either with AIROF [9] or SIROF [18] iridium valency is most likely +3 at potentials close to the reversible potential for hydrogen evolution. Figure 7 has been constructed assuming that this valency occurs at -0.2 V. In the same figure we have presented the curve achieved from the cyclic voltammogram of Figure 1 by averaging the charge exchanged during the positive and negative going scans. A slight shift is observed between the two curves

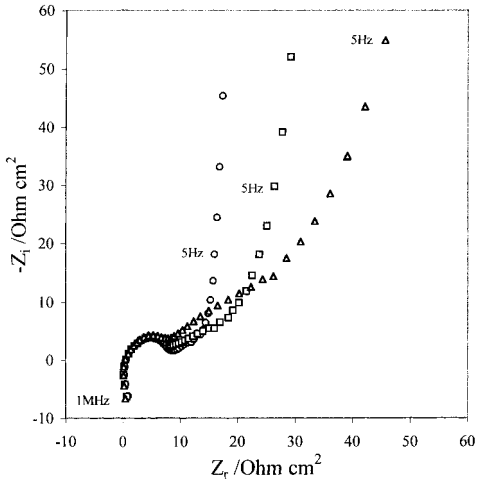

Fig. 5. Nyquist plots in the high frequencies range after R_s subtraction for various potentials. Key: (○) 0.4 V, (□) 0.2 V and (△) 0.0 V vs SCE.

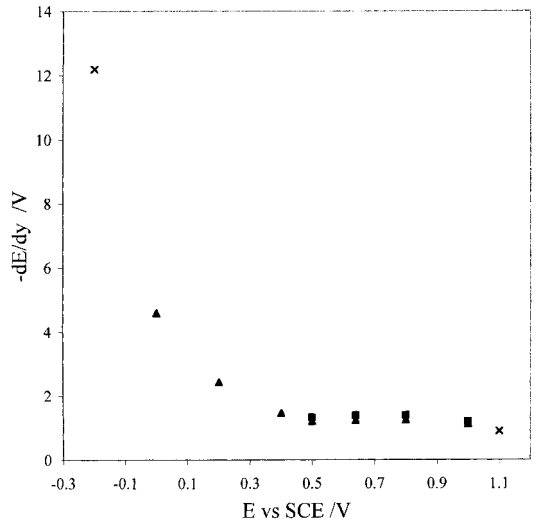

Fig. 6. Variation of $(-dE/dy)$ against potential and history (the cross shaped points are related to complementary measurements carried out with another sample). First point recorded at rest potential (◆), before (■) and after (▲) cycling.

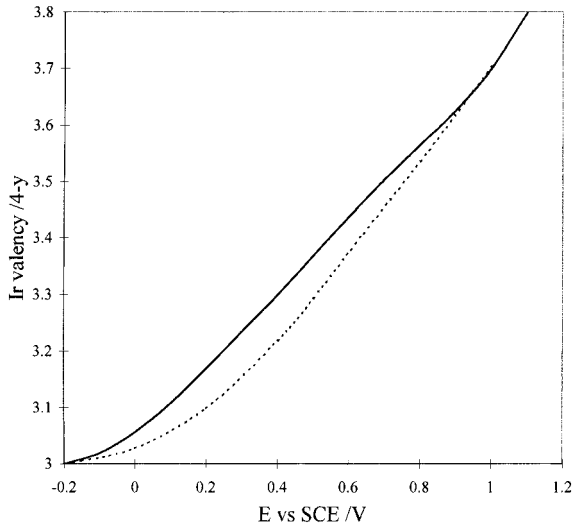

Fig. 7. Variation of iridium valency in SIROF against potential in 1 M H_2SO_4. Solid line: average value from the positive and negative going scans in cyclic voltammograms; dashed line: from impedance data.

at the lowest potentials but they overlap beyond 0.9 V. At 1.1 V, the insertion number y is about 0.2.

The chemical diffusion coefficient of hydrogen can be calculated between 0.4 and 1 V from the Warburg coefficient, W, with help of the relation:

$$\tilde{D}_H = \left[\frac{v_{IrO_2}\left(-\frac{dE}{dy}\right)}{FSW}\right]^2 \qquad (5)$$

v_{IrO_2} is a function of the density of the film and is hence different for noncycled and cycled films with respective density values of 10 and 7.8 $g\,cm^{-3}$. The results are presented in Figure 8. Universally, between 0.4 and 1 V, $\tilde{D}_H$ ranges from 2×10^{-8} to $1.1 \times 10^{-7}\,cm^2\,s^{-1}$ respectively. We have not found data in literature which may be compared to these values, although they are consistent with the short response time of SIROF during charge transfer and optical density transient reported in [14] and the short time for equilibration of the film. In Figure 8, $\tilde{D}_{app}$ has also been reported and corresponds to the values obtained precluding the change in film density. The CB treatment leads to a significant increase of $\tilde{D}_H$, especially conspicuous at the rest potential, 0.64 V, with a fourfold higher value in the final state (from 2×10^{-8} to $8 \times 10^{-8}\,cm^2\,s^{-1}$). Considering the change in film thickness, the response time to a small potential step of an electrochromic device should to be divided by 2.4 with the CB treatment. Hackwood et al. [12] found an increase of one order of magnitude from charge response measurements but after applying large potential steps between alternatively 0 and 1 V. Universally, the motion of hydrogen in the film is facilitated after hydration.

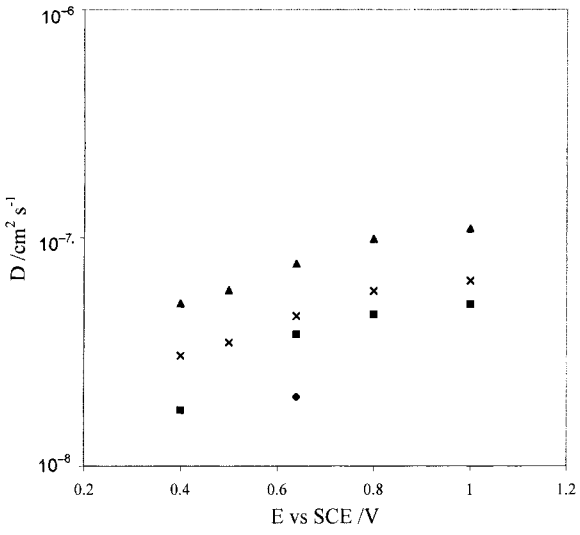

Fig. 8. Variation of $\tilde{D}_H$ and $\tilde{D}_{app}$ (×) in SIROF against potential and history. First point recorded at rest potential (◆), before (■) and after (▲) cycling.

Another interesting feature of Figure 8 is that $\tilde{D}_H$ reproducibly depends on the applied potential, and therefore on the oxidation state of iridium. When E varies from 1 to 0.4 V (y from 0.30 to 0.78), the coefficient significantly decreases from 1.1×10^{-7} to $7 \times 10^{-8}\,cm^2\,s^{-1}$. This variation is likely due to a gradual saturation of the most accessible sites for hydrogen in the compound.

The variations of the Warburg coefficient observed in AIROFs are fundamentally different from those reported here. Glarum and Marshall [4] found a considerable variation of this parameter corresponding to an increase in the diffusion coefficient greater than 10^4 between 0.4 and 1 V. They concluded that the 'coth' term was not attributable to the restricted diffusion of a species but to the a.c. response of a very highly porous film with oxide sites accessible to the electrolyte and reacting with protons in solution. The hypothesis was in agreement with previous data and observations concluding to the porous nature of AIROFs [21]. Aurian-Blajeni et al. [7] used another equivalent circuit with a CPE element behaving in sulfuric acid like a Warburg element. In this media, they found an increase in the diffusion coefficient by three orders of magnitude over the potential range mentioned above. The variation was interpreted as due to a change in the conducting species depending on the redox state of AIROF. The transport of charge was assumed to be limited by electrons in the reduced state and limited by protons in the oxidized one.

As already mentioned the impedance spectra recorded below 0.4 V were difficult to fit with a $A\coth(j\omega u)^{1/2}/(j\omega u)^{1/2}$ term over the intermediate frequency range. This particular shape can not be interpreted as due to the occurrence of a migration phenomenon at these potentials because the fall in conductivity of SIROF during bleaching is limited: values of 300 and 40 $S\,cm^{-1}$ are reported in the literature for coloured and bleached states respectively [14, 25]. In contrast, AIROFs are poorly conducting in the bleached state, with a conductivity of about $10^{-2}\,S\,cm^{-1}$ at 0.4 V

[4]. In Figure 6, between 0.4 and −0.2 V, a significant increase in $-dE/dy$ by an order of magnitude is observed. These observations suggest that further interfacial phenomena may occur over this potential range, although they can not be clarified from the data presented here or those reported in the literature.

From the Nernst–Einstein equation and the relationship between the diffusion coefficient of protons and the hydrogen chemical diffusion coefficient [26], the partial conductivity due to protons is expressed by [27]

$$\sigma_{H^+} = \frac{F\tilde{D}_H}{v_{IrO_2}}\left(-\frac{dE}{dy}\right)^{-1} \quad (6)$$

The results are presented in Figure 9. The behaviour with potential and history is similar to that of $\tilde{D}_H$ because the slope of y against potential does not significantly change over this potential range. The order of magnitude of σ_{H^+} is $2\text{–}4 \times 10^{-5}\,S\,cm^{-1}$ and this is very small compared to the total conductivity of the sample. Impedance data confirm that SIROFs are mainly electronic conductors with a very low ionic conductivity due to proton motion. This is one of the applicability requirements of the model used here for Z_d analysis [27] because in this case the potential is a function of hydrogen activity in the sample.

4. Conclusions

Sputtered iridium oxide films have been studied by impedance spectroscopy in the potential range where a change of colour from transparent to grey–black is observed. The results show that at the higher potentials investigated, between 0.4 and 1 V vs SCE, the spectra can be fitted with an equivalent circuit corresponding to an electrochemical insertion. The parameters of the circuit have been extracted as a function of potential before and after a colouring–bleaching treatment. No significant change of the kinetic parameter is observed during the experiment, whereas a strong variation of hydrogen transport properties of the films occurs. The chemical diffusion coefficient of hydrogen decreases significantly with the amount of inserted hydrogen because of the saturation of accessible sites. Moreover, $\tilde{D}_H$ significantly increases with hydration, that is, after the CB treatment. We have confirmed that SIROFs are mainly electronic conductors: the protonic conductivity values have an order of magnitude of $10^{-5}\,S\,cm^{-1}$ to be compared with total conductivities ranging between 40 and $300\,S\,cm^{-1}$. Impedance spectroscopy measurements corroborate that the valency of iridium depends on the applied potential and varies between 3 to 3.8 for applied potentials ranging between −0.2 and 1.1 V. Below 0.4 V, a change in the shape of the impedance spectra is observed in the intermediate frequency range. This is probably due to a change in the interfacial reactivity but requires further investigation.

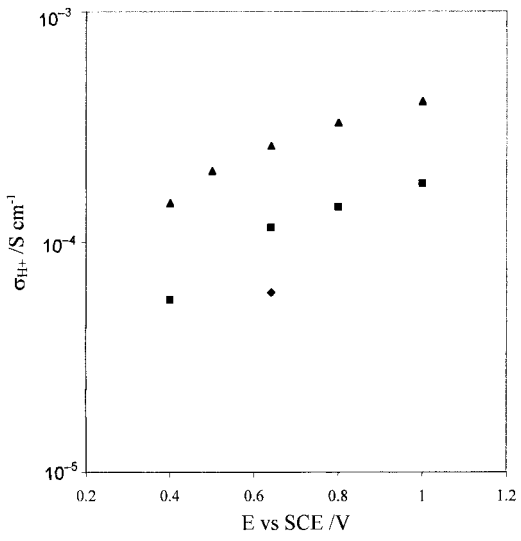

Fig. 9. Variation of the partial conductivity due to protons in SIROF with potential and history. First point recorded at rest potential (◆), before (■) and after (▲) cycling.

Acknowledgement

The authors wish to acknowledge C. Lefrou, who supplied the SIROF samples while she was at Saint-Gobain Recherche.

References

1. S. Gottesfeld, J.D.E. McIntyre, G. Beni and J.L. Shay, *Appl. Phys. Lett.* **33** (1978) 208.
2. S. Gottesfeld and J.D.E. McIntyre, *J. Electrochem. Soc.* **126** (1979) 742.
3. J.D.E. McIntyre, W.F. Peck and S. Nakahara, *J. Electrochem. Soc.* **127** (1980) 1264.
4. S.H. Glarum and J.H. Marshall, *J. Electrochem. Soc.* **127** (1980) 1467.
5. R. Kötz, H. Neff and S. Stucki, *J. Electrochem. Soc.* **131** (1984) 72.
6. J.D.E. McIntyre, S. Basu, W.F. Peck, W.L. Brown and W.M. Augustyniak, *Phys. Rev. B* **25** (1982) 7242.
7. B. Aurian-Blajeni, X. Beebe, R.D. Rauth and T.L. Rose, *Electrochim. Acta* **34** (1989) 795.
8. R. Kötz, C. Barbero and O. Hass, *J. Electroanal. Chem.* **296** (1990) 37.
9. M. Hüppauff and B. Lengeler, *J. Electrochem. Soc.* **140** (1993) 598.
10. L.M. Schiavone, W.C. Dautremont-Smith, G. Beni and J.L. Shay, *Appl. Phys. Lett.* **35** (1979) 823.
11. L.M. Schiavone, W.C. Dautremont-Smith, G. Beni and J.L. Shay, *J. Electrochem. Soc.* **128** (1981) 1339.
12. S. Hackwood, W.C. Dautremont-Smith, G. Beni, L.M. Schiavone and J.L. Shay, *J. Electrochem. Soc.* **128** (1981) 1212.
13. W.C. Dautremont-Smith, L.M. Schiavone, S. Hackwood, G. Beni and J.L. Shay, *Solid State Ionics* **2** (1981) 13.
14. S. Hackwood, G. Beni and P.K. Gallagher, *Solid State Ionics* **2** (1981) 297.
15. K.S. Kang and J.L. Shay, *J. Electrochem. Soc.* **130** (1981) 766.
16. S. Hackwood, A.H. Dayem and G. Beni, *Phys. Rev. B* **26** (1982) 471.
17. M. Bardin, P. Loheac, M. Petit, V. Plichon and N. Richard, *New J. Chem.* **19** (1995) 59.
18. T. Pauporté, D. Aberdam, J.L. Hazemann, R. Faure and R. Durand, *J. Electroanal. Chem.* **465** (1999) 88.

19. K. Yamanaka, *Jpn J. Appl. Phys.* **28** (1989) 632.
20. M.A. Petit and V. Plichon, *J. Electroanal. Chem.* **444** (1998) 247.
21. J.D.E. McIntyre, *J. Electrochem. Soc.* **129** (1982) 1269.
22. T. Pauporté, F. Andolfatto and R. Durand, *Electrochim. Acta*, in press.
23. R. DeLevie, *in* 'Advances in Electrochemistry and Electrochemical Engineering', edited by P. Delahay, Vol. 6 (J.Wiley &Sons, New York, 1967), p. 330.
24. C. Ho, I.D. Raistrick and R.A. Huggins, *J. Electrochem. Soc.* **127** (1980) 343.
25. M. Hernandez, PhD thesis, University Bordeaux I, Bordeaux (1998).
26. H. Rickert and H.D. Wiemhöfer, *Solid State Ionics* **11** (1983) 257.
27. W. Weppner and R.A. Huggins, *J. Electrochem. Soc.* **124** (1977) 1569.